Combined Experimental and Theoretical Study on the Reductive Cleavage of Inert C−O Bonds with Silanes: Ruling out a Classical Ni(0)/Ni(II) Catalytic Couple and Evidence for Ni(I) Intermediates

Josep Cornella,[†] Enrique Gómez-Bengoa,*[,‡] and Ruben Martin*[,†]

[†]Institute of Chemical Research of Catalonia (ICIQ), Av. Països Catalans 16, 43007, Tarragona, Spain
[‡]Department of Organic Chemistry I, Universidad País Vasco, UPV/EHU, Apdo. 1072, 20080, San Sebastian, Spain

Ⓢ *Supporting Information*

ABSTRACT: A mechanistic and computational study on the reductive cleavage of C−OMe bonds catalyzed by Ni(COD)$_2$/PCy$_3$ with silanes as reducing agents is reported herein. Specifically, we demonstrate that the mechanism for this transformation does not proceed via oxidative addition of the Ni(0) precatalyst into the C−OMe bond. In the absence of an external reducing agent, the in-situ-generated oxidative addition complexes rapidly undergo β-hydride elimination at room temperature, ultimately leading to either Ni(0)−carbonyl- or Ni(0)−aldehyde-bound complexes. Characterization of these complexes by X-ray crystallography unambiguously suggested a different mechanistic scenario when silanes are present in the reaction media. Isotopic-labeling experiments, kinetic isotope effects, and computational studies clearly reinforced this perception. Additionally, we also found that water has a deleterious effect by deactivating the Ni catalyst via formation of a new Ni-bridged hydroxo species that was characterized by X-ray crystallography. The order in each component was determined by plotting the initial rates of the C−OMe bond cleavage at varying concentrations. These data together with the in-situ-monitoring experiments by ^{1}H NMR, EPR, IR spectroscopy, and theoretical calculations provided a mechanistic picture that involves Ni(I) as the key reaction intermediates, which are generated via comproportionation of initially formed Ni(II) species. This study strongly supports that a classical Ni(0)/Ni(II) for C−OMe bond cleavage is not operating, thus opening up new perspectives to be implemented in other related C−O bond-cleavage reactions.

INTRODUCTION

In recent years, the use of phenol derivates as aryl C(sp^2)−O electrophiles in cross-coupling reactions have emerged as a high cost-effective and environmentally friendly alternative to aryl halide counterparts.[1,2] Among their advantages is that halide waste is avoided and that phenols are more readily available than the corresponding aryl halides.[2] Despite the advances realized, the use of C(sp^2)−O electrophiles is rather limited to its sulfonate, carbamates, carbonates, esters, or phosphate derivatives (Scheme 1, left).[1] This is probably due to their remarkable ability to act as leaving groups, thus facilitating the oxidative addition step within the catalytic cycle. Unfortunately, however,

all these methodologies are not yet entirely attractive from an atom-economical point of view due to generation of large amounts of byproduct waste and the need for derivatization of the starting phenol. Therefore, the use of more attractive C−O electrophiles that would meet these challenges will be highly desirable. In this regard, activation of C(sp^2)−OMe bonds is particularly attractive (Scheme 1, right) due to the fact that (a) aryl methyl ethers are commercially available and inexpensive building blocks and (b) aryl methyl ethers are the simplest derivatives from phenols, thus becoming the most atom- and step-economical counterparts in the phenol series.[3]

Unlike the use of other C(sp^2)−O electrophiles, catalytic cross-coupling reactions based upon cleavage of C(sp^2)−OMe bonds are still scarce.[4,5] Indeed, chemists have the general perception that C(sp^2)−OMe bonds are rather inert, as illustrated by the fact that the vast majority of metal-catalyzed reactions perfectly tolerate the presence of aryl methyl ethers.[2] Not surprisingly, the few existing methodologies for C(sp^2)−OMe bond cleavage mostly utilize highly reactive organometallic species in stoichiometric amounts to overcome the remarkable

**Scheme 1. C−O Electrophiles in Cross-Coupling Reactions**
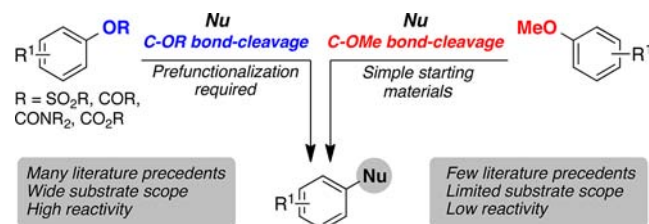
activation energy required for $C(sp^2)-OMe$ cleavage.[4,5] Although no mechanistic studies have been conducted for C—OMe bond-cleavage reactions,[6] it is believed that all these methodologies follow a classical catalytic cycle consisting of an initial oxidative addition, transmetalation, and final reductive elimination (Scheme 2).[4,5]

Scheme 2. Accepted Mechanism for C—OMe Cleavage
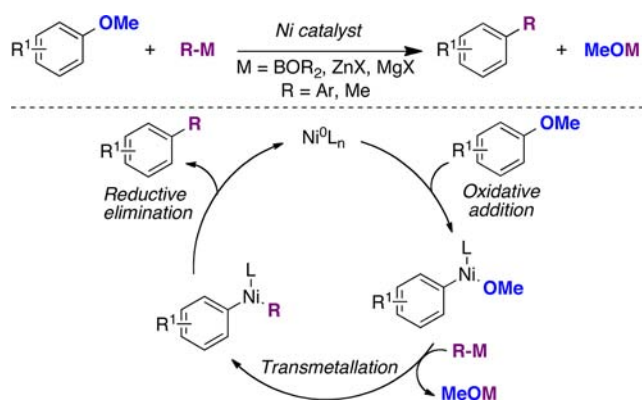
Recently, we reported a Ni-catalyzed reductive cleavage of C—OMe bonds[7] using TMDSO[8] as hydride donor (Scheme 3).[9,10]

Scheme 3. Ni-Catalyzed Reductive C—OMe Cleavage
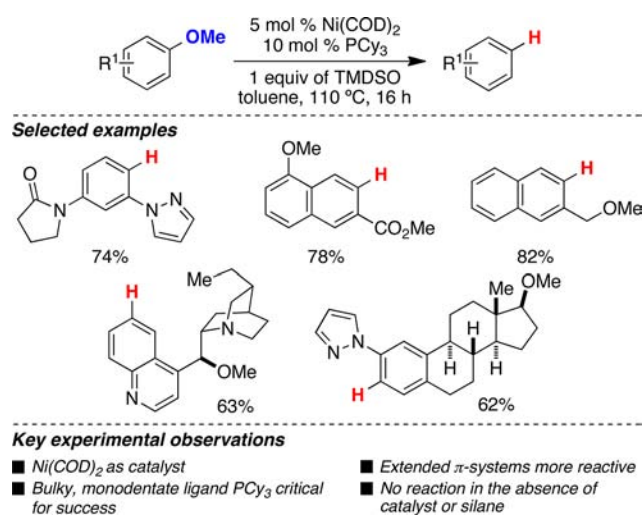
As for other C—O bond-cleavage reactions, the use of PCy_3 was found to be the most critical factor for success.[5] Shortly after, Chatani and Tobisu[11] independently described a related Ni-catalyzed procedure of aryl methyl ethers and aryl pivaloates using $(MeO)_2MeSiH$ as the reducing agent. Subsequently, Hartwig reported a Ni-catalyzed protocol that reductively cleaved $C(sp^2)-OAr$ and some C—OAlkyl bonds in the presence of H_2.[12] Overall, this recent literature data clearly illustrates the prospective impact of this methodology in the field of homogeneous catalysis.[13,14] Our catalytic protocol based on the use of TMDSO was characterized by its wide substrate scope and excellent chemoselectivity profile, allowing for coupling of a wide variety of aryl methyl ethers with a different set of substitution patterns (Scheme 3).[7] Our methodology was found to preferentially activate $C(sp^2)-OMe$ bonds in the presence of $C(sp^3)-OMe$ bonds, allowing for site-selectivity approaches in

more complex organic frameworks such as quinine or estradiol-type backbones (Scheme 3, bottom).[7]

Intriguingly, our Ni-catalyzed reaction of aryl methyl ethers with silanes exhibited unexpected reactivity depending on the catalyst and/or substrates of choice:[7]

(a) Use of Ni precatalysts other than $Ni(COD)_2$ provided trace amounts of the final products.

(b) Control experiments indicated that the reaction did not proceed in the absence of catalyst or silane, thus ruling out simple nucleophilic aromatic substitution or β-hydride elimination pathways.

(c) Extended π systems gave consistently better reactivity than simple anisole derivatives.

(d) Bulky and electron-rich monodentate PCy_3 was critical for success; under our reaction conditions, no other ligand, neither monodentate nor bidentate, afforded the desired coupling products, thus showing the subtleties of our catalytic protocol.

Despite the recent advances in the field,[4,5] a mechanistic understanding of the Ni-catalyzed C—OMe bond cleavage still remains elusive and speculative at this time.[6] This is likely due to in-situ formation of short-lived nickel species, which are exceptionally sensitive as compared to their Pd analogues. Recently, Agapie and co-workers reported an elegant stoichiometric, *intramolecular* mechanistic study on the Ni-mediated reductive cleavage of C—O bonds with pincer-type ligands.[15,16] However, *all bidentate or pincer-type ligands analyzed were found to be inert for the intermolecular* Ni-catalyzed cleavage of $C(sp^2)-$ OMe bonds promoted by silanes;[7,11] as indicated above, *monodentate PCy_3 was the only ligand that showed activity in a catalytic fashion.* Unlike the use of bidentate or pincer-type ligands,[17] however, the available literature data reveals limited examples in which reaction mechanisms have been studied with monodentate ligands in an *intermolecular* fashion.[18] Most likely, ligand dissociation, the presence of low-coordinate species, the lack of a driving force for preparing metal complexes, and the lower redox ability of the metal chelates as compared with the bidentate or the pincer-type backbones constitutes serious barriers for studying reaction mechanisms using monodentate ligands.

Although we anticipated that a complete mechanistic understanding for cleavage of C—OMe bonds *in an intermolecular fashion* would be far from trivial, we decided to shed light into this fast-growing and challenging area of expertise by studying the reaction mechanism with the *real catalytic system based on monodentate PCy_3 as the supporting ligand.*[7] Herein, we describe our mechanistic investigations on the Ni-catalyzed reductive cleavage of C—OMe bonds from an experimental and computational point of view. We demonstrate that, in the presence of silanes, the widely accepted mechanism for C—OMe cleavage[4,5] consisting of a Ni(0)/Ni(II) couple is not operating and that a new pathway involving Ni(I) species is responsible for the observed reactivity. We believe our results might have a significant impact in other related C—O bond-cleavage reactions, suggesting that mechanistic scenarios other than the classical Ni(0)/Ni(II) couple could be conceivable as well.

■ RESULTS AND DISCUSSION

Study of the Reactivity of Putative Reaction Intermediates and Catalyst Deactivation. Prompted by our initial results[7] and available literature data,[4−6] we formulated a working hypothesis for our Ni-catalyzed reductive cleavage of $C(sp^2)-$

OMe bonds promoted by silanes. Thus, we believed that the reaction was initiated by oxidative addition into the C(sp^2)−OMe bond (**II**), followed by σ-bond metathesis and a final reductive elimination from a Ni(II)−hydride, delivering the final product while regenerating the active Ni(PCy$_3$)$_2$ (**I**) species (Scheme 4).

Scheme 4. Initial Proposed Mechanistic Hypothesis
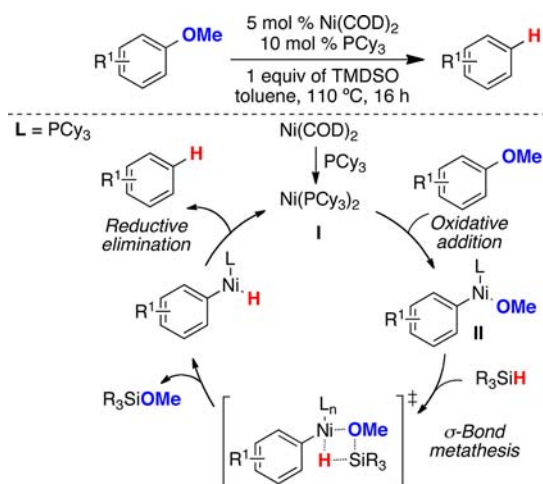
To gain insights into this mechanism, we decided to focus our attention on the oxidative addition complex **II** (Scheme 4). Beyond any reasonable doubt, a deeper understanding of the reactivity of **II** will have significant ramifications in other related C−O bond-cleavage processes described in the literature as oxidative addition has invariably been proposed to be the first step within the catalytic cycle.[4,5] Given that extended π systems have systematically been found to be much more reactive than regular anisole derivatives in C(sp^2)−OMe cleavage reactions,[4,5,7,11] we started our study with 2-methoxynaphthalene (**1**). Unfortunately, all our attempts of isolating **II** by reacting **1** with Ni(COD)$_2$/PCy$_3$ were not successful. A simple spectroscopical analysis of the crude reaction mixture revealed a significant amount of Ni(COD)$_2$, suggesting incomplete conversion to the active Ni(PCy$_3$)$_2$ species (**I**). These results questioned the simple and commonly accepted assumption that PCy$_3$ easily replaces COD under the reaction conditions,[5] arguably indicating that COD competes with substrate binding. Indeed, we performed titration experiments that showed an equilibrium between Ni(COD)$_2$ and Ni(PCy$_3$)$_2$ (**I**) by NMR spectroscopic analysis, favoring the former over the desired 14-electron species **I**.[19] While this might seem undesirable at first sight, the presence of COD in the reaction medium actually turns out to be highly advantageous as other Ni precatalysts such as NiCl$_2$ or NiCl$_2$·glyme in combination with Zn as reducing agent were not as reactive as Ni(COD)$_2$.[19] We tentatively propose that COD might indeed serve as ancillary ligand to protect the propagating and highly reactive Ni(PCy$_3$)$_2$ species **I** in the resting state of the catalyst.

In light of these observations, an indirect route for the oxidative addition species **II** was envisaged (Scheme 5). Reaction of (2-naphthyl)bis(triphenylphosphine)nickel(II) chloride **2**, easily obtained from 2-chloronaphthalene and Ni(PPh$_3$)$_4$,[20] with 2 equiv of PCy$_3$ in acetone cleanly afforded 91% of **3**.[21] Such complex was unambiguously characterized by X-ray crystallography, showing that the Ni atom is in a square-planar geometry surrounded by two phosphorus atoms in trans coordination

Scheme 5. Stoichiometric Studies
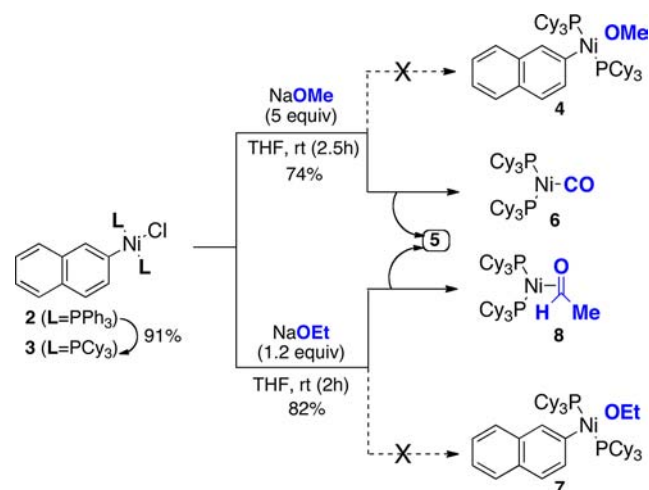
geometry (Figure 1). With substantial amounts of **3** in hand, we hypothesized that the oxidative addition species **4** could be easily
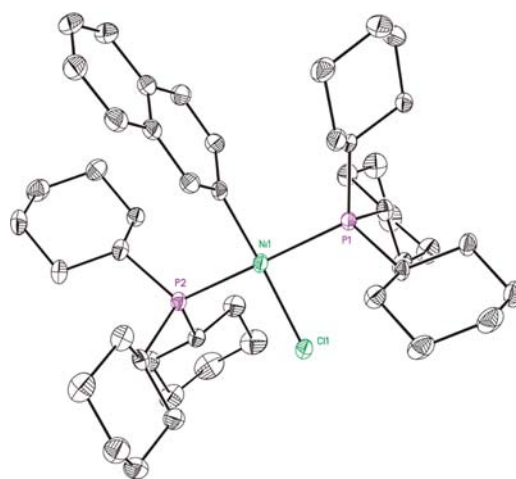

Figure 1. ORTEP diagram of **3**. Selected bond lengths (Angstroms) and angles (degrees): Ni1−Cl1, 2.2252(8); P2−Ni1, 2.2583(8); P1−Ni1, 2.2430(8); C11−Ni1, 1.927(10); C1−Ni1−P1, 174.71(9); C1−Ni1−P2, 90.10(10).

obtained by anion metathesis with NaOMe (Scheme 5, top).[22] According to our expectations, **3** was rapidly converted at room temperature in less than 2 h to a new species by treatment with NaOMe in THF.[23] Surprisingly, however, naphthalene (**5**) was formed almost quantitatively and ^{31}P NMR spectroscopic data did not match with the expected oxidative addition species **4**. The identity of this new compound was finally revealed by X-ray structure analysis. As shown in Figure 2, this complex turned out to be the symmetrical trigonal Ni(PCy$_3$)$_2$CO complex **6**. Similarly, exposure of **1** to NaOEt cleanly produced a new complex at room temperature after 2 h reaction time (Scheme 5, bottom) that did not correspond to the oxidative addition complex **7**. X-ray crystallography unambiguously identified this complex as **8** (Figure 3). In contrast to **6**, however, the molecular structure of **8** shows that an ethanal molecule is coordinated to the Ni(0) center in a η^2-fashion, resulting in a distorted tetrahedral geometry with different Ni−O and Ni−C distances (Figure 3).[24] As expected from a nonsymmetrical geometry, **8**
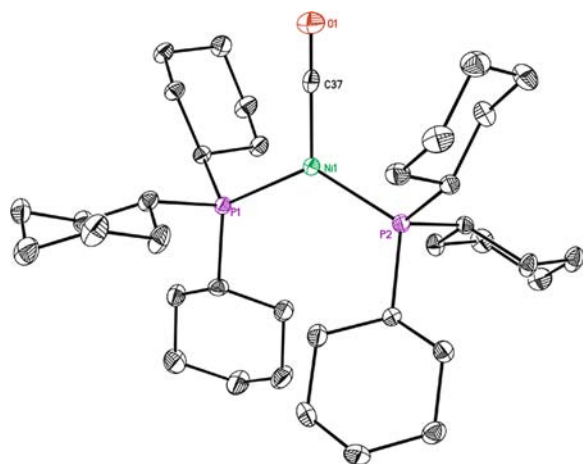
Figure 2. ORTEP diagram of **6**. Selected bond lengths (Angstroms) and angles (degrees): Ni1−C37, 1.719(5); P2−Ni1, 2.2047(7); P1−Ni1, 2.2223(7); C37−Ni1−P2, 117.09(8); Ni1−C37−O, 170(3).
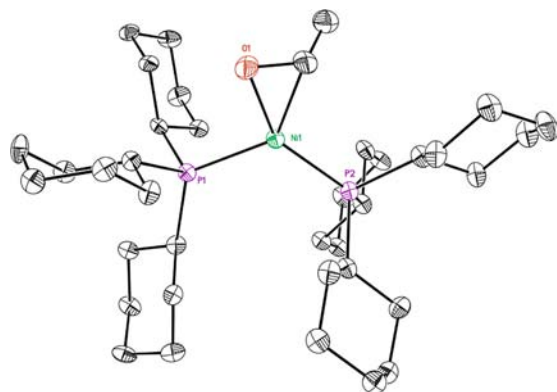

Figure 3. ORTEP diagram of **8**. Selected bond lengths (Angstroms) and angles (degrees): Ni1−P1, 2.2326(17); Ni1−P2, 2.1410(16); Ni−O1, 1.872(4); Ni1−C37, 1.933(6); C37−Ni1−P1, 133.56(18); O1−Ni1−P1, 94.30(13); O1−Ni1−C37, 40.2(2).

showed two pair of doublets at 48.5 and 35.9 ppm by ^{31}P NMR spectroscopy.

Formation of **6** and **8** is best explained by an initial halogen metathesis leading to **III**. Upon β-hydride elimination, **III** generates a naphthyl−Ni(II) hydride **IV** that rapidly undergoes reductive elimination, giving rise to naphthalene (**5**) and Ni(PCy$_3$)$_2$ that likely remains bound to the aldehyde template in a η^2-fashion (Scheme 6). Subsequently, a dehydrogenation

**Scheme 6. Mechanistic Proposal for Complexes 5 and 6**
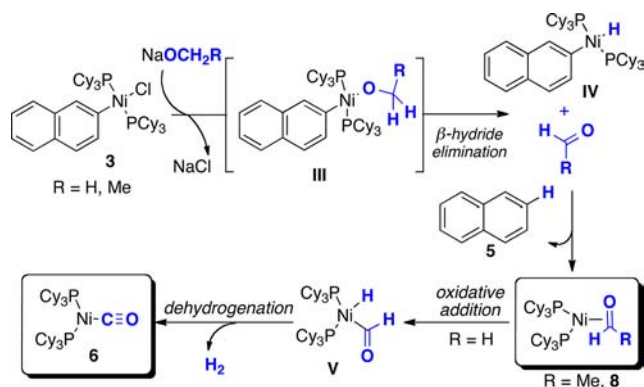
event initiated by oxidative addition into the aldehydic C−H bond ultimately leads to **6**.[25] Unlike the dehydrogenation event in route to **6**, however, extrusion of methane via decarbonylation of ethanal (R = Me) was not observed. Thus, complex **8** was isolated in analytically pure form without traces of **6** detected by NMR spectroscopy of the crude reaction mixture, even after longer reaction times. While β-hydride elimination from alkoxide-bound metal complexes has been reported in the literature with pincer-type ligands, these reactions usually required high temperatures;[15−26] it is noteworthy that in the presence of PCy$_3$, however, β-hydride elimination occurred at an exceptional rate at room temperature. These results evidence the known ability of bidentate ligands to significantly retard β-hydride elimination.[27]

The data summarized above arguably illustrate that the oxidative addition species **4** and **7** underwent β-hydride elimination with exceptional ease in the absence of silanes, even at room temperature (Scheme 5). We speculated that preparation of structurally well-characterized Ni(PCy$_3$)$_2$ (**I**) species, which are more amenable to mechanistic studies, would shed light into these intriguing observations. To such end, the known complex [Ni(PCy$_3$)$_2$]$_2$N$_2$ (**9**)[28] seemed ideally suited for our purpose as **9** generates, in situ, Ni(PCy$_3$)$_2$ in argon atmospheres. Importantly, treatment of **1** with **9** (0.50 equiv) in toluene at 100 °C afforded **5** and **6** in 54% yield in the absence of silane (Scheme 7).

Scheme 7. Reactivity of 1 with 9 in the Absence of Silane
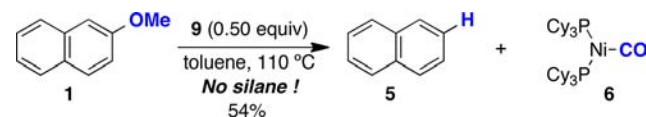

Although the data in Schemes 5 and 7 showed that β-hydride elimination pathways are indeed conceivable in a stoichiometric fashion, we believe that this particular manifold represents a minor contribution, if any, under our catalytic conditions. This assumption is supported by the fact that *not even traces of naphthalene (**5**) were observed upon exposure of **1** to our optimized catalytic protocol based upon Ni(COD)$_2$ and PCy$_3$ in the absence of silane* (Table 1, entry 1). As shown in entries 2 and 3, control experiments in the absence of Ni(COD)$_2$, PCy$_3$, or silane did not afford the desired product. Similarly, no reaction was observed in the presence of H$_2$ (entry 4).[12] In sharp contrast, addition of 1 equiv of TMDSO or 2 equiv of Et$_3$SiH afforded naphthalene in quantitative yields (entry 5). In line with the stoichiometric results in Scheme 8, use of catalytic amounts of **9** in the absence of silane resulted in non-negligible amounts of **5** (entry 6). Likewise, the behavior of Ni(PCy$_3$)$_2$(C$_2$H$_4$) (**10**)[28b] followed a similar pattern (entry 7); in this particular case, however, **5** was formed at much less extent, reinforcing the notion that ancillary ligands such as COD or ethylene might indeed play a critical role for preventing, or at least retarding, β-hydride elimination. The fact that not full conversion is achieved for both **9** and **10** precatalysts in the absence of silane (entries 6 and 7) contributes to the perception that **6**, the Ni complex that is generated upon β-hydride elimination and dehydrogenation events (Schemes 6 and 7), was not catalytically active. As expected, **6** was not a suitable Ni precatalyst under our reaction conditions. In sharp contrast, both **9** and **10** were catalytically competent in the presence of TMDSO, resulting in a 54% and 90% yield of **5**, respectively (entries 8 and 9).

Table 1. Reaction of 1 with Different Ni(0) Precatalysts[a]

entry	[Ni]	TMDSO (equiv)	GC yield (%)[b]
1	Ni(COD)$_2$/PCy$_3$	none	0
2	Ni(COD)$_2$	1	0
3	none	1	0
4[c]	Ni(COD)$_2$/PCy$_3$	none	0
5	Ni(COD)$_2$/PCy$_3$	1	99[d]
6	[(Cy$_3$P)$_2$Ni]$_2$N$_2$ (9)	0	6
7	(Cy$_3$P)$_2$Ni(C$_2$H$_4$) (10)	0	2
8	[(Cy$_3$P)$_2$Ni]$_2$N$_2$ (9)	1	54
9	(Cy$_3$P)$_2$Ni(C$_2$H$_4$) (10)	1	90
10[e]	Ni(COD)$_2$/PCy$_3$	1	5

[a]Reactions were carried out with **1** (0.25 mmol), TMDSO (0.25 mmol), and Ni(0) precatalyst (10 mol %) at 110 °C for 14 h. [b]Yields determined by GC analysis using decane as internal standard. [c]Reaction was carried out under 1 atm of H$_2$. [d]Quantitative yield was also observed when Et$_3$SiH (2 equiv) was utilized. [e]A 1 equiv amount of degassed H$_2$O was added.

Scheme 8. Isotope-Labeling Experiments
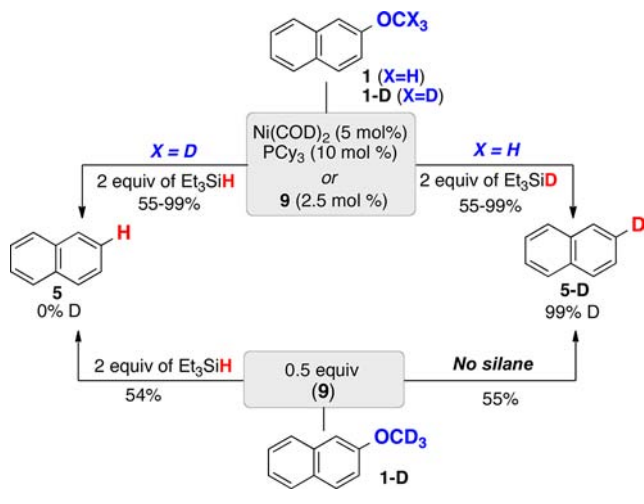
Notably, we found that that addition of 1 equiv of water to the reaction of **1** under our optimized conditions resulted in almost no conversion to **5** (Table 1, entry 10). Likewise, traces of water had also a detrimental effect in this reaction, resulting in much slower rates and lower yields of **5**.[19] Interestingly, NMR spectroscopy of the crude reaction mixtures showed significant amounts of Et$_3$SiOSiEt$_3$, suggesting catalyst decomposition in the presence of trace amounts of water. Beyond any doubt, a better understanding of this decomposition pathway would be critical for designing more efficient and improved catalysts. Gratifyingly, careful crystallization at low temperatures of a stoichiometric reaction in the presence of water furnished crystals suitable for X-ray crystal structure analysis, in which the Ni(II) complex **11** was obtained (Figure 4).[29] Such complex contains two hydroxo bridging groups in addition to a naphthyl unit and PCy$_3$. While identification of **11** shows that catalyst decomposition might occur if not rigorous anhydrous conditions are utilized, its molecular structure suggests that the elusive oxidative addition species **4** might contain bridging alkoxy groups as well.[30]
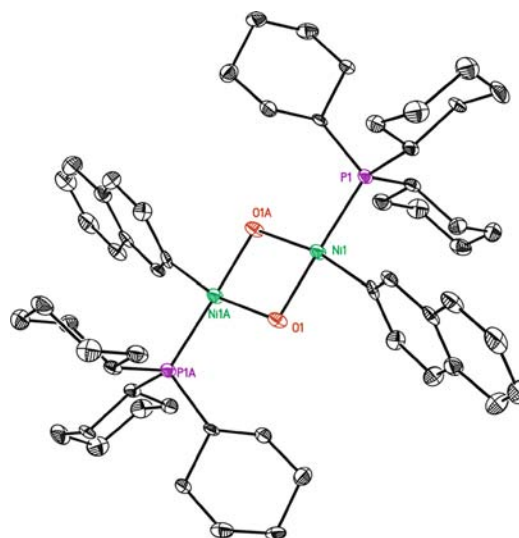

Figure 4. ORTEP diagram of **11**. Selected bond lengths (Angstroms) and angles (degrees): P1A−Ni1A, 2.1660(15); Ni1A−O1A, 1.897(17); Ni1A−C1, 1.888(4); P1A−Ni1A−O1A, 97,0(5); P1A−Ni1A−O1, 170.0(4); P1A−Ni1A−C1, 95,70(13).

Taken together, the above data show not only the striking different reactivity of Ni(0) precatalysts (Table 1) but also the deleterious effect that water might have in the reaction outcome (Figure 4).[19] The difference in reactivity is particularly pronounced with Ni(COD)$_2$ as the catalyst. The superior catalytic activity of the latter illustrates the crucial role of COD, acting as a noninnocent ancillary ligand that stabilizes the resting state of the catalyst and retards the subsequent oxidative addition step.[31] However, the ability of the oxidative addition species to rapidly undergo β-hydride elimination in the absence of silane, even at room temperature, is rather striking and certainly does not clarify the role of silane in our catalytic protocol.

Isotope-Labeling Studies and Kinetic Isotope Effects. In order to fully understand the role of the silane on the Ni-catalyzed reductive cleavage of C(sp^2)−OMe bonds we carried out isotope-labeling studies with Et$_3$SiD and **1-D** (Scheme 8).[32] If the reaction commences with oxidative addition, then one might anticipate some degree of deuterium scrambling in the product as we demonstrated that β-hydride elimination rapidly takes place at room temperature (Scheme 5). As shown in Scheme 8, exclusive formation of 2-deuteronaphthalene (**5-D**) was observed by reacting **1** with Et$_3$SiD, employing a catalytic system based upon either Ni(COD)$_2$/PCy$_3$ or **9** (99% and 55%, respectively; Scheme 8, top right). A similar argument applies for the observed opposite labeling pattern by reacting 2-deuteromethoxynaphthalene (**1-D**) with Et$_3$SiH (Scheme 8, top left). Within the limits of detection, no sign of deuterium scrambling was observed in either case. These experimental results provide strong evidence that silanes are indeed the hydride sources responsible for yielding naphthalene and that a β-hydride elimination pathway is unlikely in our catalytic protocol.

In line with our previous observations in which an ancillary ligand is not present (Scheme 7), reaction of **1-D** with stoichiometric amounts of **9** in the absence of silane delivered exclusively **5-D** (Scheme 8, bottom right); note, however, that in the presence of Et$_3$SiH, **1-D** gave rise to **5** with no traces of **5-D** being detected in the crude reaction mixture (Scheme 8, bottom left). We believe these results clearly show the intriguing

dichotomy on the reaction outcome depending on whether silanes are present or not in the reaction media.

More interestingly, no kinetic isotope effect ($k_H/k_D = 1$) was observed when comparing the initial rates of **1** with Et_3SiH and Et_3SiD, suggesting that Si−H bond cleavage is not involved in the rate-determining step;[33,34] if our initially postulated mechanism is correct (Scheme 4), the observed kinetic isotope effect together with the results shown in Scheme 8 suggested that σ-bond metathesis must proceed at a faster rate as compared to β-hydride elimination. This assumption is, however, somewhat controversial given the exceptional rate for β-hydride elimination in our stoichiometric studies, thus leaving some doubt with regard to the proposed catalytic cycle based upon an oxidative addition followed by σ-bond metathesis (Scheme 4).

Kinetic Studies: Insights into the Turnover-Limiting Step. The results in Schemes 5 and 7 together with the kinetic isotope effects suggest that our initial mechanistic hypothesis (Scheme 4) might have been premature and that further experiments would deserve more careful consideration. Convinced of the relevance of this study, we continued performing more systematic investigations in order to elucidate how silanes are involved and what their exact role is in our reductive catalytic protocol. Thus, we turned our attention to determine the order of all reaction components as it might give us valuable information about the species that are involved in the rate-determining step.

Initial rates were monitored by taking aliquots from the reaction mixture and analyzed by gas chromatography, changing the concentration of each reactant using **1** and $Ni(COD)_2/PCy_3$ as substrate and catalyst. Given the similar reactivity of TMDSO and Et_3SiH under our reaction conditions, we chose Et_3SiH as the silane source. As shown in Figures 5 and 6, the reaction

Figure 6. Plot of initial rates vs concentration of catalyst.

Figure 7. Plot of initial rates vs concentration of Et_3SiH.

it was highly informative to observe that our model reaction was partially inhibited upon increasing the naphthalene (**5**) concentration;[19] such inverse dependence implies that product **5** competes with **1** for substrate binding.

Theoretical Calculations for a Mechanism Consisting of a β-Hydride Elimination or σ-Bond Metathesis. We performed DFT calculations with the Gaussian 09 suite of programs.[35] Optimizations were carried out using the standard 6-31G(d,p) basis set for C, H, O, P, and Si and the LANL2DZ (Hay and Wadt)[36] basis including an effective core potential for Ni. Single-point calculations were performed on the optimized structures with B3LYP[37] and Truhlar's M06[38] functionals in combination with different large basis sets, like 6-311++G(d,p) for C, H, O, P, and Si atoms and SDD (Stuttgart−Dresden effective core potential)[39] for Ni, or def2-TZVPP basis set. The values reported in this work, which are given in kcal/mol, correspond to Gibbs free energies (G) and include thermal and zero-point vibrational corrections (ZPVE). When necessary, a solvent model system (IEFPCM, toluene)[40] was also included. We used $HSiMe_3$ as a computational model of $HSiEt_3$ to avoid the high conformational complexity of the latter.[41] We initially
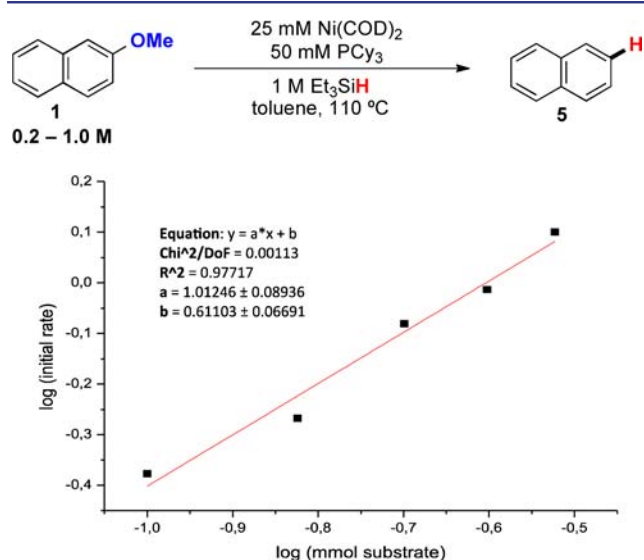

Figure 5. Plot of initial rates vs concentration of **1**.

exhibits a first-order dependence on both catalyst and substrate **1**. While these results might indeed account for oxidative addition being rate determining, the surprising first-order dependence on Et_3SiH (Figure 7) reinforces the perception that a different mechanism is operative in our reaction conditions. These striking results are in sharp contrast with the originally postulated mechanism in which oxidative addition was believed to be rate determining (Scheme 5). On the other hand,
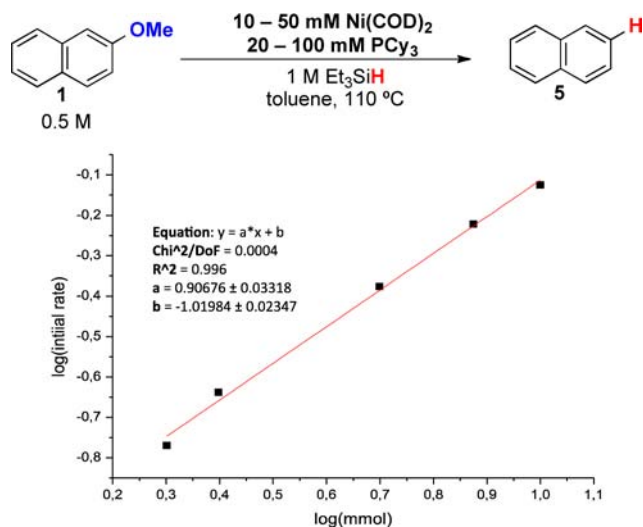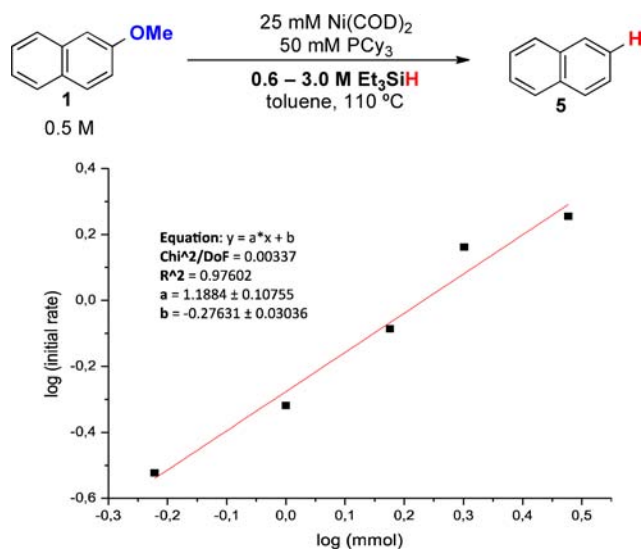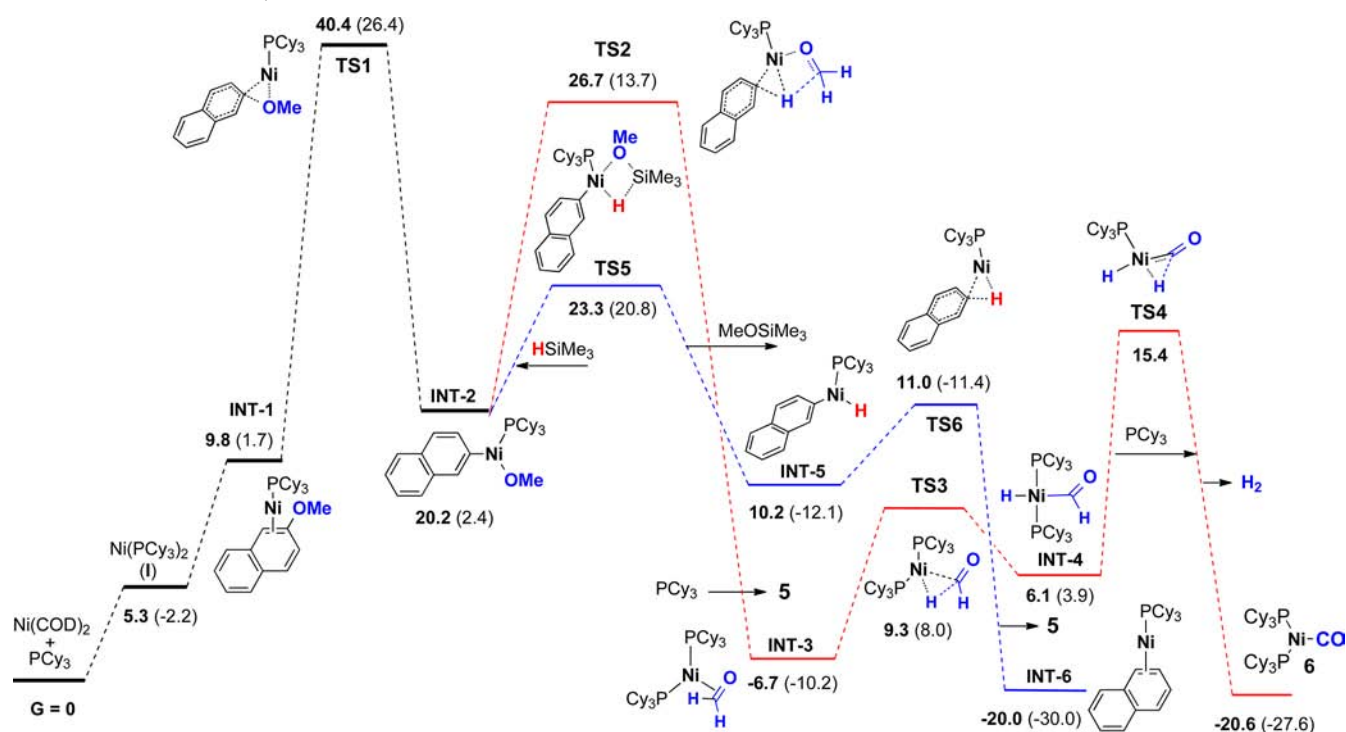
Scheme 9. Gibbs Free Energy Surfaces of the Favored Pathways for C−OMe Bond Cleavage via Oxidative Addition Followed by σ-Bond Metathesis or β-Hydride Elimination[a]

[a]Energies are in kcal/mol and calculated using M06/6-311++G**(SDD). Values in parentheses correspond to B3LYP/def2-TZVPP.

used PMe$_3$ as a simplified model of the more demanding ligand PCy$_3$; after observing divergent dissociation energy values between both phosphines, however, we decided to include PCy$_3$ in the most critical steps of the mechanism.

Our available data unambiguously suggested that a different mechanistic scenario came into play. We anticipated that computational studies would allow gathering indirect but rather important evidence for such hypothesis. Specifically, we aimed to shed light into the following striking observations: (a) no reaction is observed when utilizing a catalytic system based upon Ni(COD)$_2$/PCy$_3$ until silane is added to the reaction mixture; (b) isotope-labeling studies illustrated that the proposed σ-bond metathesis should occur at a faster rate than a β-hydride elimination pathway; (c) the lack of a kinetic isotope effect indicated that the Si−H bond was not irreversibly cleaved during the rate-determining step, and (d) the reaction showed a first-order dependence in substrate, catalyst, and silane concentration.

The controversial findings that **1** afforded cleanly naphthalene (**5**) when operating with **9** and not with our optimized protocol based upon Ni(COD)$_2$/PCy$_3$ (Scheme 7 and Table 1) prompted us to study computationally the more accessible pathway toward the putative oxidative addition species **4** depending on the catalyst of choice.

We experimentally demonstrated by titration studies that PCy$_3$ does not easily replace COD from Ni(COD)$_2$ complex to form the 14-electron Ni(PCy$_3$)$_2$ species (**I**).[19] We first computed the equilibrium energies between both Ni species and also the coordination of **1** to form **INT-1** (Scheme 9). While B3LYP showed that the equilibrium is shifted to Ni(PCy$_3$)$_2$ (**I**), M06 functional theory correctly predicted that Ni(PCy$_3$)$_2$ is 5.3 kcal/mol higher in energy than Ni(COD)$_2$ ($K_{eq} = 1.14 \times 10^{-4}$). These results corroborated that the B3LYP functional was not appropriate to predict the experimental greater stability of

Ni(COD)$_2$ as compared to Ni(PCy$_3$)$_2$ (**I**).[42] As shown in Scheme 9, displacement of the two COD ligands by **1** and PCy$_3$ is highly disfavored (**INT-1**, +9.8 kcal/mol, M06). Furthermore, oxidative addition into the C(sp^2)−OMe bond from **INT-1** had a high activation Gibbs free energy of 30.6 kcal/mol, affording a total activation barrier of 40.4 kcal/mol from Ni(COD)$_2$ to **TS1**. This high computed energy contributes to the notion that a mechanism based upon a classical oxidative addition into the C−OMe bond using Ni(COD)$_2$ as precatalyst is highly unlikely (Scheme 4). In sharp contrast, the M06 functional predicted an activation barrier of 35.1 kcal/mol for oxidative addition from Ni(PCy$_3$)$_2$ (**TS1**), making such process feasible at high temperatures. This is in agreement with the experimental observation that [Ni(PCy$_3$)$_2$]$_2$N$_2$ (**9**) facilitates oxidative addition at 110 °C (Scheme 7). Once again, B3LYP failed to predict this experimental evidence[43] as oxidative addition from Ni(COD)$_2$ has a remarkable low activation Gibbs free energy of 26.4 kcal/mol from Ni(COD)$_2$ (**TS1**). It is worth noting that the dissociation energy values obtained for PMe$_3$ or PCy$_3$ toward formation of Ni(PR$_3$)$_2$ are different enough to discourage the use of PMe$_3$ as a valid model of PCy$_3$, at least regarding comparison of Ni species of different coordination number.

We next studied the ability of the key oxidative addition intermediate **INT-2** to form naphthalene (**5**), in both the absence or the presence of silane (Scheme 9). Intermediate **INT-2** bears a coordination vacancy that can serve both to accommodate the forming hydride in the β-elimination event (absence of silane) or to coordinate the silane and promote the σ-bond metathesis process. In the absence of silane (Scheme 9, red lines) we confirmed computationally that the transformation of **INT-2** into **5** follows an exothermic pathway through a series of low-energetic transition states, namely, β-hydride elimination (**TS2**), C−H oxidative addition (**TS3**), and α-elimination (**TS4**)

to afford naphthalene **5** and the experimentally observed $(PCy_3)_2Ni-CO$ complex **6**. In the presence of silane (Scheme 9, blue lines), the σ-bond metathesis is fast, leading to a highly reactive intermediate **INT-5** (**TS5**), which suffers an instantenous C–H bond-reductive elimination to **INT-6**. Subsequently, **INT-6** would form either $Ni(PCy_3)_2$ (**I**) or **INT-1** by coordination with either PCy_3 or **1**, respectively. In the event of a hypothetical competition between both pathways, the σ-bond metathesis process (**TS5**) has a barrier of 3.4 kcal/mol lower than the β-hydride elimination (**TS2**). These results are in line with the observed isotope-labeling studies (Scheme 8). More interestingly, both pathways should be relatively facile at room temperature as soon as **INT-2** is formed in the reaction medium. These results are in perfect agreement with the experimental observation that **3** rapidly reacts with NaOMe at room temperature, giving rise to **6** (Scheme 5).

While the M06 functional predicted that σ-bond metathesis was faster than β-hydride elimination (**TS5** vs **TS2**), there were still several inconsistencies that left some doubt about the proposed mechanism in Scheme 4: (a) the activation barrier in route to **INT-2** from $Ni(COD)_2$ was too high to be achievable under reaction conditions based upon $Ni(COD)_2$ and PCy_3 (**TS1**, 40.4 kcal/mol); note, however, that the reaction can occur at some extent from $Ni(PCy_3)_2$ (**TS1**, 35.1 kcal/mol). This argument should be valid independently on whether a silane is present or not as **INT-2** is the common intermediate of both scenarios; (b) according to the theoretical calculations in Scheme 9, the silane does not participate during or before the rate-determining step (**TS1**).[44] These results are clearly inconsistent with the observed first-order dependence on silane concentration.

In-Situ Monitoring: Evidence for Ni(I) Intermediates. In view of the controversial results gathered by our kinetic and computational studies, we set out to explore and clarify in more detail the critical role of the silane in our catalytic protocol. Accordingly, we turned our attention to in situ monitor the course of a catalytic reaction of **1** with $Ni(COD)_2/PCy_3$ by gas chromatography. Interestingly, we observed that reaction with Et_3SiD evidenced a slightly longer induction period as compared with its Et_3SiH analogue, thus evidencing the critical role of silanes for generating the active propagating species.[19] In order to study in more depth the striking difference in these observed induction periods, we further monitored the model reaction by ^1H NMR spectroscopy at 100 °C in a stoichiometric fashion. Notably, we observed that rapid consumption of Et_3SiH occurred when mixing Et_3SiH (2 equiv), **1** (1 equiv), $Ni(COD)_2$ (1 equiv), and PCy_3 (2 equiv), even when naphthalene (**5**) was not yet formed. Additionally, we also monitored the reaction by ^{29}Si NMR spectroscopy during the induction period and showed no other species than unreacted Et_3SiH. Taken together, we believe these results suggest the intermediacy of paramagnetic species present in the reaction mixture. It is also worth noting that during the course of the reaction where naphthalene (**5**) was being formed the only species observed by ^{29}Si NMR were Et_3SiOMe.

To shed more light into the initial consumption of Et_3SiH at short reaction times, we also monitored the reaction by in-situ IR spectroscopy (Figure 8).[45] As expected from the observed ^1H NMR spectroscopical data, depletion of the signal corresponding to the Si–H at 812 cm^{-1} was observed (Figure 8, blue line). It is important to highlight that *during the induction period in which consumption of Et_3SiH is observed, no naphthalene (**5**) was detected* by either gas chromatography or ^1H NMR spectroscopy.
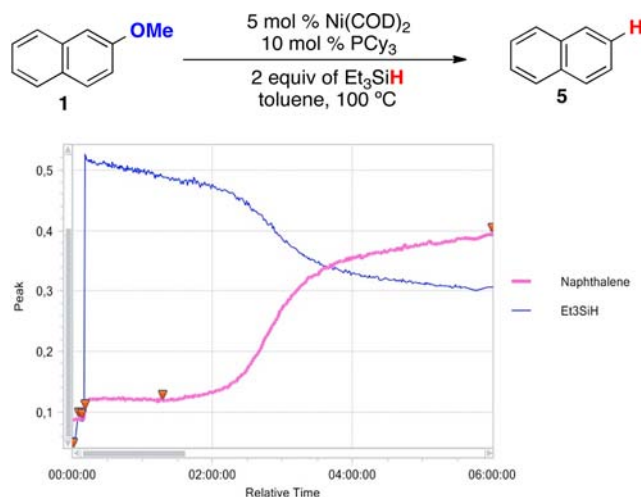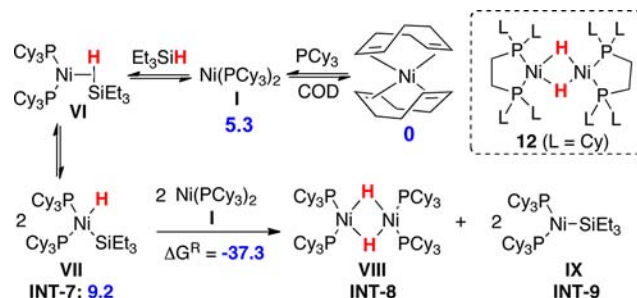

Figure 8. In-situ monitoring by FTIR spectroscopy.

On the basis of the above experimental mechanistic data, we hypothesized that at initial stages Et_3SiH might bind reversibly to $Ni(PCy_3)_2$ (**I**) in a η^2-fashion (**VI**) (Scheme 10). Related Ni

Scheme 10. Formation of Ni(I)–H and Ni(I)–SiR$_3$ Species from Ni(COD)$_2$^{a}

^{a}Gibbs free energies computed at M06/6-311++(d,p) (SDD) (blue).

complexes have previously been reported, although low temperatures are generally required due to their high instability.[46,47] We hypothesized that **VI** presumably undergoes oxidative addition into the Si–H bond, affording a Ni(II) intermediate **VII**.[48] Subsequently, a comproportionation of these species and $Ni(PCy_3)_2$ (**I**)[49] would lead to a Ni(I)–hydride (**VIII**) and Ni(I)–$SiEt_3$ (**IX**).[50] Consistent with the available literature data on related Ni(I)–hydrides, we believe that **VIII** are diamagnetic species that contain a Ni^I-Ni^I bonding interaction.[51] This hypothesis is supported by the fact that ^1H NMR spectroscopy of a crude reaction mixture showed a characteristic signal at -15.8 ppm during the course of the reaction.[19] This value is in analogy with the chemical shift of an otherwise similar Ni(I)–hydride complex **12** containing a bidentate linkage with tricyclohexylphosphine units that was prepared following a slightly modified literature procedure.[52,53] Careful crystallization from pentanes at -40 °C furnished crystals suitable for X-ray structure analysis (Figure 9).[54] Still, however, our experiments did not allow us to rule out an equilibrium of **VIII** with the corresponding monomeric and, therefore, paramagnetic Ni(I)–H species. As for Ni(I)–$SiEt_3$ species, we speculate that the steric bulk imposed by the bulky PCy_3 results in only monomeric, tricoordinated paramagnetic species **IX**.[50]

2004

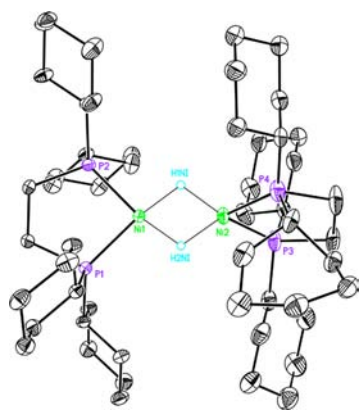dx.doi.org/10.1021/ja311940s | *J. Am. Chem. Soc.* 2013, 135, 1997–2009

Figure 9. ORTEP diagram of **12**. Selected bond lengths (Angstroms) and angles (degrees): Ni1−P1, 2.1350(7); Ni1−P2, 2.1356(7); Ni1−Ni2, 2.4078(5); P1−Ni1−P2, 91,52(3); P1−Ni1−Ni2, 133.63(2); P2−Ni1−Ni2, 134.73(2).

To gain more insight on whether paramagnetic species are present in our reaction mixture, electron paramagnetic resonance (EPR) was performed at low temperatures by taking aliquots of a stoichiometric and a catalytic reaction of **1** with Ni(COD)₂/ PCy₃ and Et₃SiH during both the induction period and at low conversions to naphthalene (**5**). Interestingly, *a characteristic EPR spectrum for Ni(I) species was obtained in all cases,*[19,55] *even after the induction period in which naphthalene (5) was being formed.* We believe these experiments advocate the notion that Ni(I) intermediates are indeed responsible for the catalytic activity in our protocol (Scheme 10).

Since our available experimental data did not allow us to rigorously distinguish whether Ni(I)−H or Ni(I)−SiR₃ was the actual propagating species, we turned our attention to theoretical calculations to confirm the role of Ni(I) intermediates in our catalytic protocol.

Theoretical Calculations for the Intermediacy of Catalytic Ni(I) Species. As shown in Scheme 10, we confirmed computationally our in-situ-monitoring studies that suggested the intermediacy of Ni(I) species (blue values). While the transformation of Ni(COD)₂ into the **INT-7** was initially disfavored, this effect was compensated by the large energy gain measured in the comproportionation event between **INT-7** and Ni(PMe₃)₂, thus rendering the Ni(I)−H dimer **INT-8** and Ni(I)−SiMe₃ species **INT-9**.[56]

In principle, two different mechanisms could be envisioned depending on the Ni(I) source. The high stability of the Ni(I)−H dimer (**INT-8**, Scheme 11) suggested that the reaction should be initiated via monomeric Ni(I)−H species **INT-10**. Subsequently, displacement of PCy₃ by 2-methoxynaphthalene (**1**) would render a new Ni(I) species (**INT-11**). At this stage, several potential pathways could be conceivable for reaction of **INT-11** with the aromatic backbone, including σ-bond metathesis or oxidative addition across the C−OMe bond, among others.[19] Among these, the lowest activation energies corresponded to Ni−H insertion into the naphthyl ring[57] (**TS7**, 18.1 kcal/mol from **INT-11**) to form a reactive intermediate, wherein the Ni(I) center and the methoxy group are positioned in contiguous carbons in an anti fashion.

We located a transition state (**TS8**) in which the Ni(I) atom migrates from the α- to the β-position of the naphthyl ring, hence triggering elimination of methanol from the β-carbon (Scheme

Scheme 11. Formation of Naphthalene (5) via Catalytic Ni(I)−H Species[a]
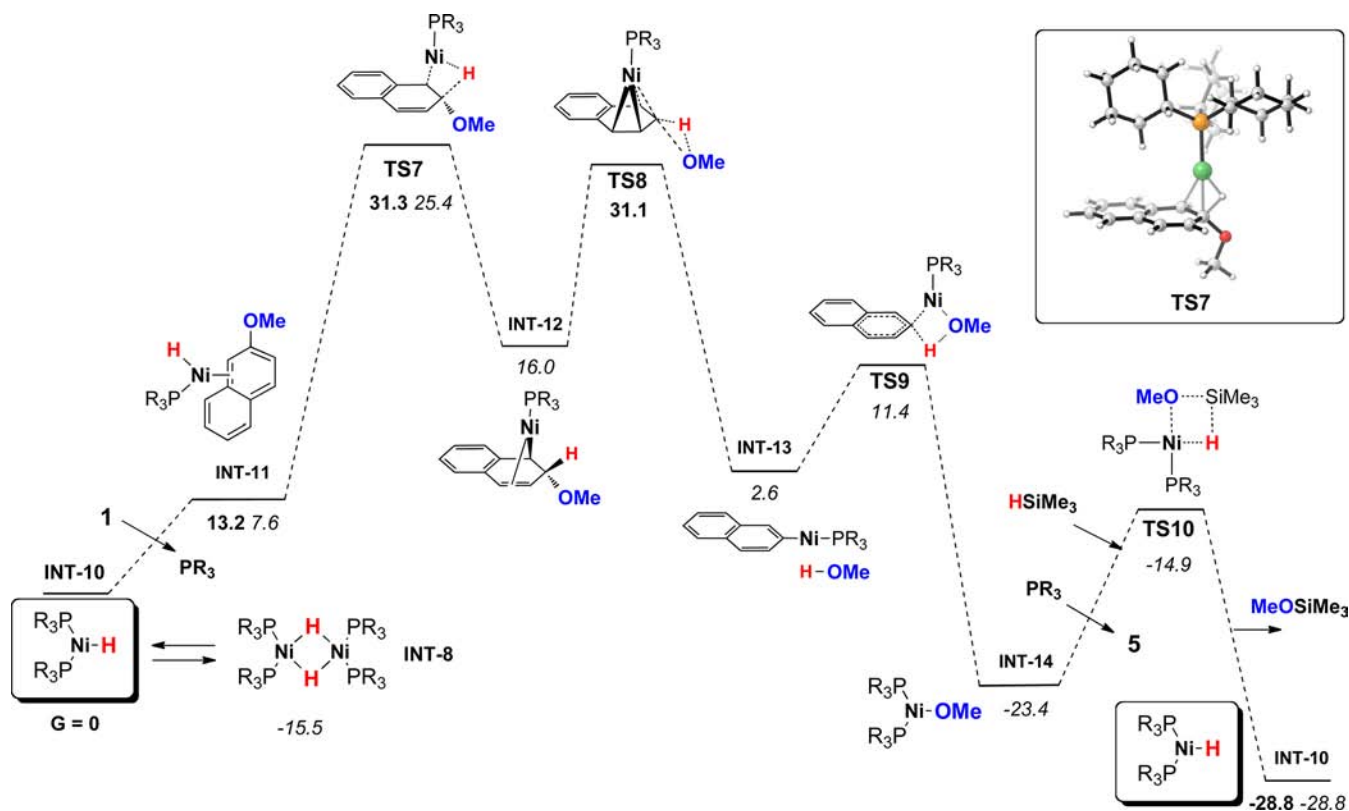
[a]Gibbs free energies calculated at M06/6-311++G(d,p) (SDD). Bold values correspond to PCy₃ and values in italic to PMe₃.

Scheme 12. Formation of Naphthalene Through Ni(I)−SiR₃ Species[a]
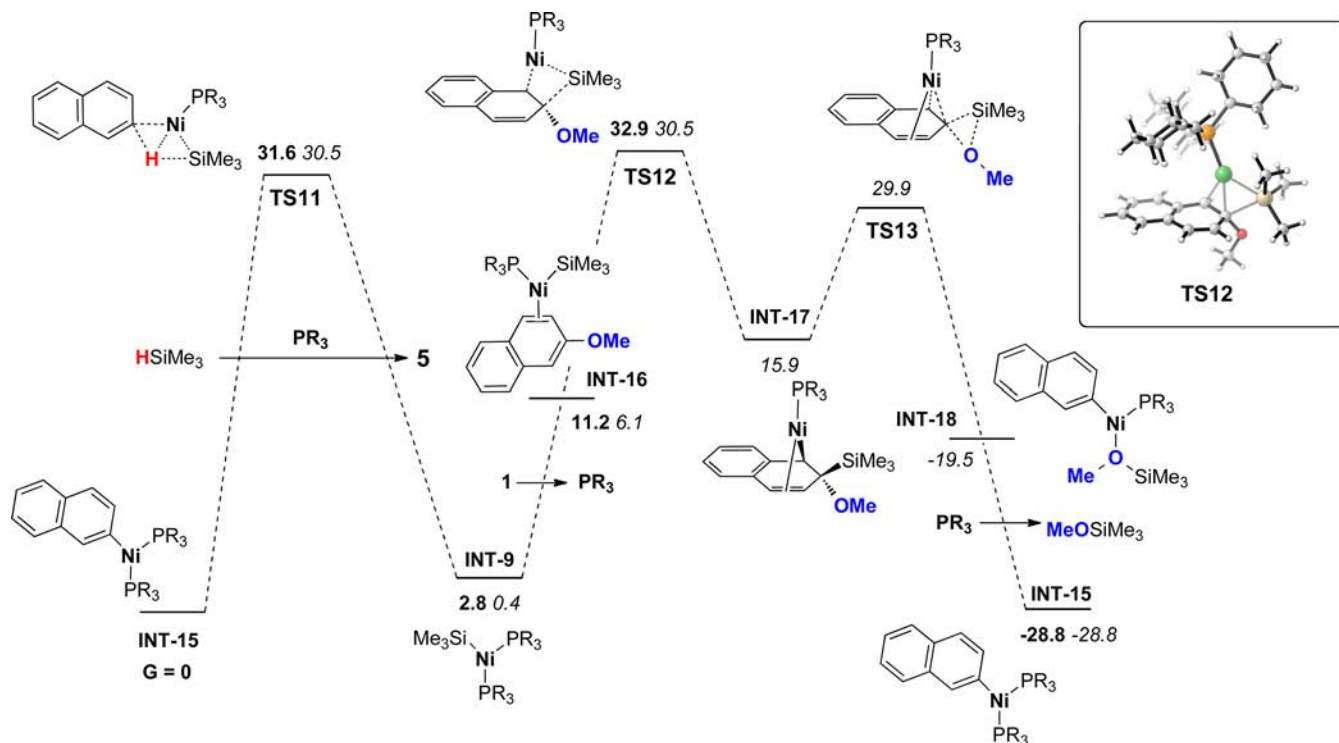
[a]Gibbs free energies calculated at M06/6-311++G(d,p) (SDD). Bold values correspond to PCy₃ and values in italic to PMe₃.

11). It is worth noting that a substantial amount of negative charge is developed in **TS8**; while this is, not surprisingly, penalized in the gas phase, a solvent model was applied to acquire a more accurate energy, rendering a value of 31.1 kcal/mol, which is of similar magnitude to **TS7**. The reaction further evolves by forming (PCy₃)₂Ni−OMe (**INT-14**), which reacts with silane through a low in energy σ-bond metathesis-type transition state **TS10**, thus recovering back the catalyst **INT-10**. It is worth noting that although we computed the full scheme with PMe₃ as the ligand, we checked the critical points with PCy₃ and confirmed that similar conclusions can be drawn for both phosphines. Nevertheless, we believe the accuracy of these results does not have any influence in the mechanism due to the following: (a) (R₃P)₂Ni(I)−H dimers (**INT-8**) are remarkably more stable than the corresponding monomeric (R₃P)₂Ni(I)−H species (**INT-10**). As judged by the calculations using PMe₃, this seemingly simple transformation is heavily penalized by the 15.5 kcal/mol difference (Scheme 11, bottom left). (b) Ni−H and Si−H bonds are broken and formed during the rate-determining step **TS7** (or **TS8**), thus suggesting that a positive kinetic isotope effect should have been observed; as already demonstrated (see above), this was not the case. (c) The silane does not participate during or before the rate-determining step; and therefore, it is not consistent with the first-order dependence on silane concentration (Figure 7).

According to the results shown in Scheme 11, we concluded that our protocol for cleavage of aryl methyl ethers in the presence of silanes could not operate under a catalytic regime based upon Ni(I)−H species. Therefore, we next turned our attention to a mechanistic alternative in which Ni(I)−SiR₃ species participate in the catalytic cycle (Scheme 12). As for the Ni(I)−H catalytic proposal (Scheme 11), the lowest energy pathway corresponded to the Ni(I)−SiR₃ bond insertion from

INT-16 into the naphthyl ring with an activation energy of 21.7 kcal/mol (Scheme 12, **TS12**). The intermediate **INT-17** then evolves by MeOSiMe₃ elimination and Ni(I) migration to form **INT-18** that easily incorporates an additional ligand on its structure to afford **INT-15**. Subsequently, **INT-15** undergoes a reversible σ-bond metathesis (**TS11**), thus giving rise to naphthalene (**5**) and recovering back the Ni(I)−SiR₃ species **INT-9**.

As shown in Scheme 12, it becomes apparent that the migratory insertion into the naphthalene backbone represents the rate-determining step of the reaction (**TS12**, 32.9 kcal/mol operating with PCy₃). Significantly, the lowest energy intermediate of the proposed mechanism does not correspond to the initial Ni(I)−SiR₃ species (**INT-9**) but rather the 2-naphthyl−Ni(I)(PCy₃)₂ complex (**INT-15**). As a result, the latter can formally be considered the resting state of the catalytic cycle. Taking a closer look into the mechanism shown in Scheme 12, our results also suggest that both 2-methoxynaphthalene (**1**) and the silane actively participate from the lowest reaction intermediate (**INT-15**) to the highest data point of the catalytic cycle (**TS12**). Such assumption cannot be underestimated as it virtually explains, for the first time, the observed first-order dependence on both **1** and Et₃SiH. Moreover, no Ni−H or Si−H is broken or formed during the rate-determining step (**TS12**), an observation that is in perfect in agreement with the lack of kinetic isotope effect when comparing the initial rates of R₃SiH vs R₃SiD. Additionally, the means to dearomatize an arene ring at the rate-determining step (**TS12**) nicely explains the greater reactivity of extended π systems as compared to simpler anisole derivatives.[4,5,7,11]

As a result and taking into consideration all the experimental data and theoretical calculations, we believe that the mechanism from which our reaction operates is initiated by Ni(I)−SiEt₃

(IX)[50] that are generated from $Ni(COD)_2$, PCy_3, and Et_3SiH via a comproportionation event (Scheme 13). Such assumption

Scheme 13. Mechanistic Proposal
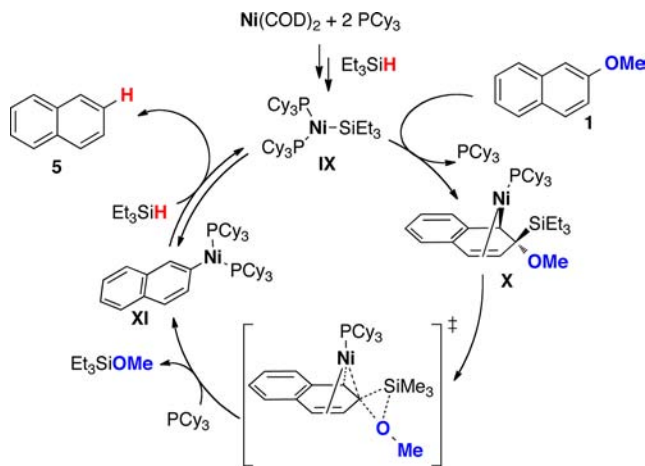
exploits a previously unrecognized opportunity in which Ni(I)−$SiEt_3$ (**IX**) are the key catalytic species, therefore constituting an opportunity for research in other fields of expertise. We believe that initially generated **IX** coordinates to **1** in a η^2-fashion and after a migratory insertion event, a benzyl nickel species **X** is generated (Scheme 13). Elimination of $MeOSiR_3$ with concomitant migration of the Ni atom results in **XI** that undergo a reversible σ-bond metathesis, delivering the final product **5** while generating back the Ni(I)−$SiEt_3$ species **IX**.

Homogeneous vs Heterogeneous Catalysis. We next focused our attention to study whether heterogeneous catalysts could be responsible for the observed catalytic activity.[58] To such end, we turned our attention to mercury poisoning experiments[59] since suppression of catalytic activity in the presence of Hg(0) is generally indicative of heterogeneous catalysis via forming an amalgam with the metal(0) heterogeneous catalysts. Interestingly, we observed that reaction of **1** with Et_3SiH was shut down in the presence of mercury under our optimized reaction conditions (Figure 10). Care must be taken in interpreting these results, as a control experiment revealed that mercury reacts with
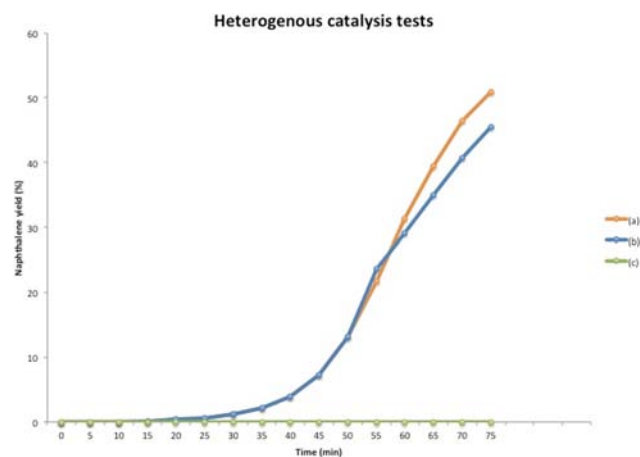

Figure 10. Plot of naphthalene (**5**) GC yield vs time from reaction of **1** with Et_3SiH (a) under the exact optimized reaction conditions (red), (b) upon filtration after 50 min reaction time, and (c) in the presence of Hg from the beginning.

$Ni(COD)_2$ in solution, thus leaving some doubt about the accuracy of such test in our protocol.[60,61] Additionally, we found that upon filtration of the mixture after 50 min reaction time, further conversion to naphthalene (**5**) was observed in a linear relationship over time (Figure 10b);[19] interestingly, no induction period was observed, suggesting the presence of homogeneous catalysts in the reaction mixture. Nevertheless, at present we cannot completely rule out a leaching from heterogeneous species, thus acting as a reservoir of the corresponding Ni homogeneous active species. In addition, TEM and ESEM analysis of different aliquots during the course of the reaction revealed formation of Ni−P particles with an average size of 200−2000 nm.[19] Arguably, such particle size rules out the intermediacy of Ni nanoparticles and suggests that if Ni−aggregates are present, these likely coexist in equilibrium with the homogeneous catalysts.[62]

■ CONCLUSIONS

This study provides compelling experimental and computational evidence that the reported Ni-catalyzed C−OMe bond-cleavage reactions occur along more than one pathway depending on the catalyst of choice. We demonstrate that the presence of ancillary ligands such as COD or ethylene play an important, if not critical, role in the reaction outcome, hence stabilizing the resting state of the catalyst and therefore retarding the subsequent oxidative addition event. On the contrary, the absence of ancillary ligands makes oxidative addition feasible. This later premise is corroborated by the unusual molecular structures **6** and **8**, unambiguously indicating that in-situ-formed alkoxy-bound Ni complexes are able to rapidly undergo at room temperature β-hydride elimination in the absence of ancillary ligand. The fact that **6** and **8** are not catalytically competent contributed to the perception that β-hydride elimination was not responsible for the catalytic activity. Additionally, isolation of **11** showed that decomposition pathways might compete with the desired catalytic transformation under nonrigorous anhydrous conditions.

Isotope-labeling studies, kinetic experiments, as well as computational studies univocally demonstrated that our Ni-catalyzed protocol for cleavage of C−O bonds with silanes as reducing agents does not operate via putative Ni(II)−oxidative addition complexes. The first-order dependence on silane concentration as well as the observed silane depletion in the induction period suggested that a distinctive mechanism came into play. In-situ monitoring by NMR and EPR spectroscopy identified the presence of Ni(I) species that are likely generated by a comproportionation event. Computational and experimental studies suggested Ni(I)−SiR_3 as the key propagating species with migratory insertion into the naphthalene backbone being the rate-determining step. Such assumption is in perfect analogy with all the recorded kinetic data, isotope-labeling studies, and the significantly greater reactivity of extended π systems as compared with simpler anisole derivatives.

Although additional investigations are warranted to expand the scope and improve even further the catalytic performance, we believe this study represents a significant step toward understanding the cleavage of inert C−O bonds in a catalytic fashion. Additionally, our investigations study, for the first time, the Ni-catalyzed C−O bond cleavage employing the catalytically active monodentate PCy_3 in an intermolecular fashion. Overall, our data suggest that related intermolecular catalytic C−O bond-cleavage reactions might indeed operate by mechanisms other than the classical Ni(0)/Ni(II) couple. We anticipate that our

study will lead to new knowledge in catalyst design, thus opening up new perspectives and stimulating new concepts within the field of C−O bond-cleavage reactions.

■ ASSOCIATED CONTENT

Ⓢ Supporting Information
Experimental procedures, spectral data, and crystallographic data (CIF); complete ref 34; computational details, Cartesian coordinates, and energies of all located structures. This material is available free of charge via the Internet at http://pubs.acs.org.

■ AUTHOR INFORMATION

Corresponding Author
rmartinromo@iciq.es; enrique.gomez@ehu.es

■ ACKNOWLEDGMENTS

■ REFERENCES

(1) For selected reviews, see: (a) Rosen, B. M.; Quasdorf, K. W.; Wilson, D. A.; Zhang, N.; Resmerita, A.-M.; Garg, N. K.; Percec, V. *Chem. Rev.* **2011**, *111*, 1346. (b) Li, B.-J.; Yu, D.-G.; Sun, C.-L.; Shi, Z.-J. *Chem.—Eur. J.* **2011**, *17*, 1728. (c) Yu, D.-G.; Li, B.-J.; Shi, Z.-J. *Acc. Chem. Res.* **2010**, *43*, 1486.

(2) In *Metal-catalyzed Cross-Coupling Reactions*; Diederich, F.; Stang, P. J., Eds.; Wiley-VCH: New York, 1998.

(3) For Ni-catalyzed cross-coupling of phenoxy derivatives, see: (a) Yu, D.-G.; Li, B.-J.; Zheng, S.-F.; Guan, B.-T.; Wang, B.-Q.; Shi, Z.-J. *Angew. Chem., Int. Ed.* **2010**, *49*, 4566. (b) Yu, D.-G.; Shi, Z.-J. *Angew. Chem., Int. Ed.* **2011**, *50*, 7097.

(4) For Ru-catalyzed C(sp²)−OMe arylation, see: (a) Ueno, S.; Mizushima, E.; Chatani, N.; Kakiuchi, F. *J. Am. Chem. Soc.* **2006**, *128*, 16516. (b) Kakiuchi, F.; Usui, M.; Ueno, S.; Chatani, N.; Murai, S. *J. Am. Chem. Soc.* **2004**, *126*, 2706.

(5) For Ni-catalyzed C(sp²)−OMe arylation methodologies, see: (a) Wang, C.; Ozaki, T.; Takita, R.; Uchiyama, M. *Chem.—Eur. J.* **2012**, *18*, 3482. (b) Wang, Z.-X.; Xie, L.-G. *Chem.—Eur. J.* **2011**, *17*, 4972. (c) Shimasaki, T.; Konno, Y.; Tobisu, M.; Chatani, N. *Org. Lett.* **2009**, *11*, 4890. (d) Tobisu, M.; Shimasaki, T.; Chatani, N. *Angew. Chem., Int. Ed.* **2008**, *47*, 4866. (e) Guan, B.-T.; Xiang, S.-K.; Wu, T.; Sun, Z.-P.; Wang, B.-Q.; Zhao, K.-Q.; Shi, Z.-J. *Chem. Commun.* **2008**, 1437. (f) Tobisu, M.; Shimasakai, T.; Chatani, N. *Angew. Chem., Int. Ed.* **2008**, *47*, 4866. (g) Dankwart, J. W. *Angew. Chem., Int. Ed.* **2004**, *43*, 2428. (h) Wenkert, E.; Michelotti, E. L.; Swindell, C. S. *J. Am. Chem. Soc.* **1982**, *104*, 1670.

(6) For a computational study dealing with C−OAc bond cleavage, see: Li, Z.; Zhang, S.-L.; Fu, Y.; Guo, Q.-X.; Liu, L. *J. Am. Chem. Soc.* **2009**, *131*, 8815.

(7) Alvarez-Bercedo, P.; Martin, R. *J. Am. Chem. Soc.* **2010**, *132*, 17352.

(8) TMDSO = 1,1,3,3-tetramethyldisiloxane.

(9) For selected reviews: (a) Ng, S.-S.; Ho, C.-Y.; Schleicher, K. D.; Jamison, T. F. *Pure. Appl. Chem.* **2008**, *80*, 929. (b) Montgomery, J. *Acc. Chem. Res.* **2000**, *33*, 467.

(10) For a related C−SMe bond-cleavage procedure, see: Barbero, N.; Martin, R. *Org. Lett.* **2012**, *14*, 796.

(11) Tobisu, M.; Yamakawa, K.; Shimasaki, T.; Chatani, N. *Chem. Commun.* **2011**, *47*, 2946.

(12) Sergeev, A. G.; Hartwig, J. F. *Science* **2011**, *332*, 439.

(13) Tobisu, M.; Chatani, N. *ChemCatChem.* **2011**, *3*, 1410. (b) McGlaken, G. P.; Clarke, S. L. *ChemCatChem.* **2011**, *3*, 1260.

(14) For examples using stoichiometric metal species (a) Azzena, U.; Dettori, G.; Idini, M. V.; Pisano, L.; Secchi, G. *Tetrahedron* **2003**, *59*, 7961. (b) Casado, F.; Pisano, L.; Farriol, M.; Gallardo, I.; Marquet, J.; Melloni, G. *J. Org. Chem.* **2000**, *65*, 322. (c) Dabo, P.; Cyr, A.; Lessard, J.; Brossard, L.; Ménard, H. *Can. J. Chem.* **1999**, *77*, 1225. (d) Maercker, A. *Angew. Chem., Int. Ed.* **1987**, *26*, 972.

(15) Kelly, P.; Lin, S.; Edouard, G.; Day, M. W.; Agapie, T. *J. Am. Chem. Soc.* **2012**, *134*, 5480.

(16) For other stoichiometric hydrogenolysis of alkoxy metal complexes with pincer-type ligands, see: (a) Fulmer, G. R.; Herndon, A. N.; Kaminsky, W.; Kemp, R. A.; Goldberg, K. I. *J. Am. Chem. Soc.* **2011**, *133*, 17713. (b) Fulmer, G. R.; Muller, R. P.; Kemp, R. A.; Goldberg, K. I. *J. Am. Chem. Soc.* **2009**, *131*, 1346.

(17) For selected reviews: (a) van Leeuwen, P. W. N. M.; Kamer, P. C. J.; Claver, C.; Pàmies, O.; Diéguez, M. *Chem. Rev.* **2011**, *111*, 2077. (b) Selander, N.; Szabó, K. J. *Chem. Rev.* **2011**, *111*, 2048. (c) Choi, J.; MacArthur, A. H. R.; Brookhart, M.; Goldman, A. S. *Chem. Rev.* **2011**, *111*, 1761. (d) van der Boom, M. E.; Milstein, D. *Chem. Rev.* **2011**, *111*, 1759.

(18) For a selection of mechanistic studies using monodentate phosphines, see: (a) Tan, Y.; Barrios-Landeros, F.; Hartwig, J. F. *J. Am. Chem. Soc.* **2012**, *134*, 3683. (b) García-Melchor, M.; Fuentes, B.; Lledós, A.; Casares, J. A.; Ujaque, G.; Espinet, P. *J. Am. Chem. Soc.* **2011**, *133*, 13519. (c) Liu, Z.; Yamamichi, H.; Madrahimov, S. T.; Hartwig, J. F. *J. Am. Chem. Soc.* **2011**, *133*, 2772. (d) Alexanian, E. J.; Hartwig, J. F. *J. Am. Chem. Soc.* **2008**, *130*, 15627. (e) Biscoe, M. R.; Barder, T. E.; Buchwald, S. L. *Angew. Chem., Int. Ed.* **2007**, *46*, 7232. (f) Macgregor, S. A.; Roe, D. C.; Marshall, W. J.; Bloch, K. M.; Bakhmutov, V. I.; Grushin, V. V. *J. Am. Chem. Soc.* **2005**, *127*, 15304.

(19) See Supporting Information for details.

(20) Zeller, A.; Herdtweck, E.; Strassner, T. *Eur. J. Inorg. Chem.* **2003**, *9*, 1802.

(21) Retbøll, M.; Edwards, A. J.; Rae, A. D.; Willis, A. C.; Bennett, M. A.; Wenger, E. *J. Am. Chem. Soc.* **2002**, *124*, 8348.

(22) For some selected references dealing with salt metathesis using bidentate ligands, see: (a) Breitenfeld, J.; Scopelliti, R.; Hu, X. *Organometallics* **2012**, *31*, 2128. (b) Mrutu, A.; Dickie, D. A.; Goldberg, K. I.; Kemp, R. A. *Inorg. Chem.* **2011**, *50*, 2729. (c) Vechorkin, O.; Csok, Z.; Scopelliti, R.; Hu, X. *Chem.—Eur. J.* **2009**, *15*, 3889.

(23) The reaction was found to be slower when stoichiometric amounts of NaOMe were used. In any case, the product of oxidative addition **4** was observed.

(24) For related η^2-bound Ni(0) carbonyl compounds prepared by other means, see: (a) Ohashi, M.; Saijo, H.; Arai, T.; Ogoshi, S. *Organometallics* **2010**, *29*, 6534. (b) Tamaki, T.; Nagata, M.; Ohashi, M.; Ogoshi, S. *Chem.—Eur. J.* **2009**, *15*, 10083. (c) Ogoshi, S.; Arai, T.; Ohashi, M.; Kurosawa, H. *Chem. Commun.* **2008**, 1347.

(25) A similar pathway has been observed for pincer-type ligands, see ref 15.

(26) For selected references, see: (a) Matas, I.; Campora, J.; Palma, P.; Alvarez, E. *Organometallics* **2009**, *28*, 6515. (b) van der Boom, M. E.; Liou, S.-Y.; Ben-David, Y.; Shimon, L. J. W.; Milstein, D. *J. Am. Chem. Soc.* **1998**, *120*, 6531. (c) Gambarotta, S.; Floriani, C.; Chiesi-Villa, A.; Guastini, C. *Organometallics* **1986**, *5*, 2425. (d) Bianchini, C.; Meli, A.

Organometallics **1985**, *4*, 1537. For a review dealing with alcoxy metal species, see: Bryndza, H. E.; Tam, W. *Chem. Rev.* **1988**, *88*, 1163.

(27) Hartwig, J. F. *Inorg. Chem.* **2007**, *46*, 1936.

(28) (a) Jolly, P. W.; Jonas, K.; Krüger, C.; Tsay, Y.-H. *J. Organomet. Chem.* **1971**, *33*, 109. (b) Aresta, M.; Nobile, C. F.; Sacco, A. *Inorg. Chim. Acta* **1974**, *12*, 167.

(29) Analytically pure **11** was only obtained in trace amounts (<5% yield) after recrystallization.

(30) Carmona, E.; Marin, J. M.; Palma, P.; Paneque, M.; Poveda, M. L. *Inorg. Chem.* **1989**, *28*, 1895.

(31) For an example, see: Fürstner, A.; Majima, K.; Martin, R.; Krause, H.; Kattnig, E.; Goddard, R.; Lehmann, W. *J. Am. Chem. Soc.* **2008**, *130*, 1992.

(32) Taking into consideration that TMDSO and Et$_3$SiH were equally effective for promoting the Ni-catalyzed reductive cleavage of C−OMe bonds, we decided to employ for our isotope-labeling studies commercially available Et$_3$SiH and Et$_3$SiD

(33) (a) Simmons, E. M.; Hartwig, J. F. *Angew. Chem., Int. Ed.* **2012**, *51*, 3066. (b) Gómez-Gallego, M.; Sierra, M. A. *Chem. Rev.* **2011**, *111*, 4857.

(34) Reaction of **1** with Ni(COD)$_2$ (5 mol %), PCy$_3$ (10 mol %), and Et$_3$SiH:Et$_3$SiD (1:1, 2 equiv) gave rise to **5** and **5-D** (1:1 ratio)

(35) For a full reference of Gaussian-09, see Supporting Information.

(36) (a) Hay, P. J.; Wadt, W. R. *J. Chem. Phys.* **1985**, *82*, 270. (b) Wadt, W. R.; Hay, P. J. *J. Chem. Phys.* **1985**, *82*, 284. (c) Hay, P. J.; Wadt, W. R. *J. Chem. Phys.* **1985**, *82*, 299.

(37) (a) Lee, C.; Yang, W.; Parr, R. G. *Phys. Rev. B* **1988**, *37*, 785. (b) Becke, A. D. *J. Chem. Phys.* **1993**, *98*, 5648. (c) Kohn, W.; Becke, A. D.; Parr, R. G. *J. Phys. Chem.* **1996**, *100*, 12974.

(38) Zhao, Y.; Truhlar, D. G. *Theor. Chem. Acc.* **2008**, *120*, 215.

(39) (a) Fuentealba, P.; Preuss, H.; Stoll, H.; Szentpaly, L. V. *Chem. Phys. Lett.* **1982**, *89*, 418. (b) Szentpaly, L. V.; Fuentealba, P.; Preuss, H.; Stoll, H. *Chem. Phys. Lett.* **1982**, *93*, 555.

(40) (a) Cancès, E.; Mennucci, B.; Tomasi, J. *J. Chem. Phys.* **1997**, *107*, 3032. (b) Cossi, M.; Barone, V.; Mennuci, B.; Tomasi, J. *Chem. Phys. Lett.* **1998**, *286*, 253. (c) Tomasi, J.; Mennucci, B.; Cancès, E. *J. Mol. Struct. (THEOCHEM)* **1999**, *464*, 21.

(41) No significant differences in free activation energies were observed when computing Et$_3$SiH vs Me$_3$SiH.

(42) B3LYP has been shown to underestimate the dissociation energies of PCy$_3$ in other organometallic complexes, see: Zhao, Y.; Truhlar, D. G. *J. Chem. Theory Comput.* **2009**, *5*, 324.

(43) For this reason, only M06 values will be used for the mechanistic discusion. B3LYP values are collected in the Supporting Information

(44) These results are in sharp contrast with the proposed mechanism for cleavage of C−OAc bonds (ref 6) in which transmetalation and not oxidative addition is rate determining.

(45) Similar experiments were performed for other reductive cleavage protocols, see: Baxter, R. D.; Montgomery, J. *J. Am. Chem. Soc.* **2011**, *133*, 5728.

(46) For selected references, see: (a) Tanabe, M.; Yumoto, R.; Osakada, K.; Sanji, T.; Tanaka, M. *Organometallics* **2012**, *31*, 6787. (b) Beck, R.; Johnson, S. A. *Organometallics* **2012**, *31*, 3599. (c) Tanabe, M.; Yumoto, R.; Osakada, K. *Chem. Commun.* **2012**, *48*, 2125. (d) Takaya, J.; Iwasawa, N. *Dalton Trans.* **2011**, *40*, 8814. (e) Iluc, V. M.; Hillhouse, G. L. *J. Am. Chem. Soc.* **2010**, *132*, 11890. (f) Chen, W.; Shimada, S.; Tanaka, M.; Kobayashi, Y.; Saigo, K. *J. Am. Chem. Soc.* **2004**, *126*, 8072.

(47) For a related σ-bound Ni(0) borane complex, see: Crestani, M. G.; Muñoz-Hernandez, M.; Arévalo, A.; Acosta-Ramirez, A.; Garcia, J. J. *J .Am. Chem. Soc.* **2005**, *127*, 18066.

(48) Iluc, V. M.; Hillhouse, G. L. *Tetrahedron* **2006**, *63*, 7577.

(49) For selected comproportionation events in route to Ni(I) species, see: (a) Velian, A.; Lin, S.; Miller, A. J. M.; Day, M. W.; Agapie, T. *J. Am. Chem. Soc.* **2010**, *132*, 6296. (b) Phapale, V. B.; Buñuel, E.; García-Iglesias, M.; Cárdenas, D. J. *Angew. Chem., Int. Ed.* **2007**, *46*, 8790. (c) Jones, G. D.; Martin, J. L.; McFarland, C.; Allen, O. R.; Hall, R. E.; Haley, A. D.; Brandon, R. J.; Konovalova, T.; Desrochers, P. J.; Pulay, P.; Vicic, D. A. *J. Am. Chem. Soc.* **2006**, *128*, 13175.

(50) For isolation of three-coordinate Ni(I)−silyl complexes, see: Iluc, V. M.; Hillhouse, G. L. *J. Am. Chem. Soc.* **2010**, *132*, 11890.

(51) (a) Minidola, D. J.; Hillhouse, G. L. *J. Am. Chem. Soc.* **2001**, *123*, 4623. (b) Vicic, D. A.; Jones, W. D. *J. Am. Chem. Soc.* **1997**, *119*, 10855.

(52) Jonas, K.; Wilke, G. *Angew. Chem., Int. Ed.* **1970**, *9*, 312. We found that **12** was not catalytically competent in our reaction protocol.

(53) For selected applications of Ni(I)−H dimers utilizing bidentate backbones, see: (a) Smith, E. E.; Du, G.; Fanwick, P. E.; Abu-Omar, M. M. *Organometallics* **2010**, *29*, 6527. (b) Torres-Nieto, J.; Brennessel, W. W.; Jones, W. D.; Garcia, J. J. *J. Am. Chem. Soc.* **2009**, *131*, 4120. (c) García, J. J.; Brunkan, N. M.; Jones, W. D. *J. Am. Chem. Soc.* **2002**, *124*, 9547. (d) Edelbach, B. L.; Lachicotte, R. J.; Jones, W. D. *Organometallics* **1999**, *18*, 4040.

(54) The structure of **12** was discussed in ref 52, but no X-ray crystallography was shown.

(55) Our results are in analogy with other Ni(I) complexes, see, for example: (a) Uyeda, C.; Peters, J. C. *Chem. Sci.* **2013**, *4*, 157. (b) Klein, A.; Vicic, D. A.; Biewer, C.; Kieltsch, I.; Stirnat, K.; Hamacher, C. *Organometallics* **2012**, *31*, 5334. (c) Kraikivskii, P. B.; Saraev, V. V.; Meusinger, R.; Bocharova, V. V.; Ushakov, I. A.; Petrovskii, S. K. *J. Organomet. Chem.* **2012**, *715*, 43. (d) Bai, G.; Wei, P.; Stephan, S. W. *Organometallics* **2005**, *24*, 5901. (e) Holland, P. L.; Cundari, T. R.; Perez, L. L.; Eckert, N. A.; Lachicotte, R. J. *J. Am. Chem. Soc.* **2002**, *124*, 14416.

(56) Unfortunately, the Ni(I)−H dimer with PCy$_3$ is not computationally tractable, as it contains four PCy$_3$ and more than 200 atoms

(57) For a Ni(I)−H insertion into arene motifs, see: Lin, S.; Day, M. W.; Agapie, T. *J. Am. Chem. Soc.* **2011**, *133*, 3828.

(58) For very recent heterogeneous Ni-catalyzed reductive cleavage of C−OAr bonds, see: (a) Sergeev, A. G.; Hartwig, J. F. *J. Am. Chem. Soc.* **2012**, *134*, 20226. (b) Parsell, T. H.; Owen, B. C.; Klein, I.; Jarrell, T. M.; Marcuum, C. L.; Hupert, L. J.; Amundson, L. M.; Kenttämaa, H. I.; Ribeiro, F.; Miller, J. T.; Abu-Omar, M. M. *Chem. Sci.* **2013**, *4*, 806. (c) He, J.; Zhao, C.; Lercher, J. A. *J. Am. Chem. Soc.* **2012**, *134*, 20768.

(59) (a) Crabtree, R. H. *Chem. Rev.* **2012**, *112*, 1536. (b) Widegren, J. A.; Finke, R. G. *J. Mol. Catal. A* **2003**, *198*, 317. (c) Yu, K. Q.; Sommer, W.; Weck, M.; Jones, C. W. *J. Catal.* **2004**, *226*, 101. (d) Foley, P.; Dicosimo, R.; Whitesides, G. M. *J. Am. Chem. Soc.* **1980**, *102*, 6713.

(60) For similar discrepancies regarding the Hg drop test reacting with homogeneous catalysts, see: Stein, J.; Lewis, L. N.; Gao, Y.; Scott, R. A. *J. Am. Chem. Soc.* **1999**, *121*, 3693.

(61) For a selected number of references that leave some doubt about the Hg drop test for identifying whether heterogeneous systems are present or not in other homogeneous reactions, see: (a) Esfandiari, N. M.; Blum, S. A. *J. Am. Chem. Soc.* **2011**, *133*, 18145. (b) Widegren, J. A.; Finke, R. G. *J. Mol. Catal. A* **2003**, *198*, 317. (c) van Asselt, R.; Elsevier, C. J. *J. Mol. Catal.* **1991**, *65*, L13. (d) Jones, R. A.; Real, F. M.; Wilkinson, G.; Galas, A. M. R.; Hurthouse, M. B. *J. Chem. Soc., Dalton Trans.* **1981**, 126.

(62) At present we cannot rule out the presence of Ni(I) clusters that are in equilibrium with their corresponding Ni(I) homogeneous monomers. Recently, related Ni(I) clusters have been reported in the literature, see: Beck, R.; Shoshani, M.; Johnson, S. A. *Angew. Chem., Int. Ed.* **2012**, *51*, 11753.